Progress in Additive Manufacturing
https://doi.org/10.1007/s40964-024-00576-2

FULL RESEARCH ARTICLE

A review of the current state-of-the-art on in situ monitoring in electron beam powder bed fusion

Marco Grasso[1] · **Bianca Maria Colosimo**[1]

Received: 30 June 2023 / Accepted: 4 February 2024

Abstract
The industrial development of electron beam powder bed fusion (PBF-EB) is relatively younger and much more limited in terms of global widespread and revenues compared to laser powder bed fusion (PBF-L). Nevertheless, PBF-EB has been adopted in some of the most successful industrial case studies of metal AM, as it provides specific benefits and capabilities that make it a key enabling technology in a variety of industrial applications. Moreover, the recent years have seen a rapid evolution with new actors and new systems entering the market, together with a considerable increase of research and innovation programs. A field of major interest is the development and continuous improvement of in situ sensing and monitoring methods to anticipate the detection of defects, to predict the final quality of the part, and to rethink product qualification procedures. The technological features of the PBF-EB process have motivated the development of solutions that differ from the ones in PBF-L. Some of them have reached a good maturity level, being recently integrated into industrial machines, while others still deserve further research. This study explores the current state-of-the-art on in situ and in-line monitoring of the PBF-EB process, aiming to provide an up-to-date overview of the major differences with respect to PBF-L, currently available methods and their performances, as well as open issues, challenges to be tackled, and perspective for future research and industrial developments.

Keywords PBF-EB · In situ monitoring · In situ sensing · Quality prediction · Defect detection

1 Introduction

Since the development of the first Arcam machine, more than 20 years ago, and the first European certification of a biomedical implant manufactured via electron beam powder bed fusion (PBF-EB), few years later, the process has considerably evolved, the range of materials has expanded, and various success cases have been achieved. Two well-known examples are the low-pressure titanium aluminide turbine blade production for the aviation industry on the one hand, and the manufacture of metal implants and prostheses with enhanced osteointegration properties in the biomedical sector, on the other hand [19, 27]. But the PBF-EB technology has exhibited a continuous growth over the years, addressing many other market needs, involving different application fields, and enabling novel advanced manufacturing capacities. This evolution has become even more evident at global level in the last 3 to 5 years, as new machine developers have entered the marked, opening new technology innovation opportunities and fostering a wider competitiveness. For a general introduction to the PBF-EB process, the current state of technology development and its industrial applications, the reader is referred to Fu and Körner [19].

One of the great innovations enabled by additive manufacturing (AM) as a pillar of the Industry 4.0 paradigm regards the possibility to "look" at the process in a completely new way, i.e., through a variety of measurements and signals gathered on a layer-by-layer basis, throughout the whole duration of the process, while the part is being built. This capability has been pointed out to be one of the key drivers to develop smart AM systems suitable to reduce wastes and defects, while meeting the stringent quality and repeatability requirements of the industrial sectors that pull the market. In situ sensing, monitoring and control methodologies for AM processes in general, and powder bed fusion

✉ Marco Grasso
marcoluigi.grasso@polimi.it

Bianca Maria Colosimo
biancamaria.colosimo@polimi.it

[1] Dipartimento di Meccanica, Politecnico di Milano, Via La Masa 1, 20156 Milan, Italy

Published online: 11 March 2024

(PBF) in particular, represent a research field characterized by an exponential increase of the scientific literature in the last years, as well as massive investments from AM machine developers and third parties. Various authors have reviewed the large amount of studies in this field, focusing on the state-of-the-art of methods in PBF [23, 35] or other processes [41, 57], while other authors reviewed the literature on related aspects, like machine learning applied to AM [36, 59] and process control methods [32, 33]. In this framework, the literature devoted to PBF-EB is much limited compared to the one devoted to PBF-L. There are different factors behind this gap. One regards the fact that the PBF-EB is much less open to in situ sensing than its laser-based counterpart. Indeed, viewports shall be shielded from X-ray leakage and metallization, no co-axial measurement of the melt pool is available, and the very high temperature of the build limits the range of sensing devices that can be installed within the chamber. Another factor is the monopoly condition that has characterized the PBF-EB market for more than 15 years, while the PBF-L market has benefited from intense competition ever since the development of the first industrial systems. Because of this, the widespread of PBF-EB systems in research laboratories has been lesser and slower than the one of PBF-L machines. Moreover, fully open PBF-L prototypes and systems have been widely available in research laboratories as testbeds to develop and validate novel sensing and monitoring solutions, while apart from quite few isolated self-developed prototypes, the first truly open PBF-EB system has been developed only in 2017.

Despite the gap in the literature between PBF-EB and PBF-L, in situ sensing and monitoring plays a central role for both the processes, since it represents the only way to detect anomalies and defects at their onset stage, possibly allowing anticipated part suppression and/or adaptive/correction actions, as well as reducing time and costs devoted to post-process inspections. As far as PBF-EB is concerned, some solutions have reached a sufficient maturity to be adopted by machine developers as embedded or optional equipment in their own systems, while other methods still deserve further research and continuous improvements. Moreover, several open issues still need to be addressed and new development areas may be explored. The current PBF-EB market situation, characterized by a much higher competitiveness than few years ago, and by a strong demand for more stable and repeatable processes and more efficient qualification procedures, represents the playground to overcome the current limits and barriers of in situ sensing, monitoring, and control approaches presently available.

This review is aimed to present an up-to-date overview of the current state-of-the-art on in situ monitoring methodologies in PBF-EB for in-line and in situ data acquisition, anomaly detection and quality prediction. The term "in-line" refers to measurements gathered during the manufacturing process. They can be acquired either "ex-situ", i.e., by moving the part to an external measurement station before going on with the process, or "in-situ", i.e., by using on-machine sensors. This review is devoted to the latter category of methods. The purpose is to provide researchers and practitioners with a synthetic summary, classification, and discussion of all techniques currently available, their pros and cons, their limitations and potential, as well as the most relevant results achieved so far. The present paper is also conceived to highlight the major differences between PBF-L and PBF-EB in terms of in situ sensing and monitoring capabilities, and to point out the most promising perspectives for future research directions.

The paper is organized as follows. Section 2 provides an overview of the scientific literature with an analysis by year, country, and topic. Section 3 briefly reviews the major differences between PBF-L and PBF-EB processes regarding the development and implementation of in situ sensing and monitoring. Section 4 reviews the current state-of-the-art on in situ sensing and monitoring solutions in PBF-EB. Section 5 summarizes the major challenges, open issues, and future perspectives in this field. Section 6 eventually concludes the paper.

2 Overview of the scientific literature

The analysis of the scientific literature presented in this study was based on Scopus and Google Scholar databases. The search was carried out by combining a search by keyword, author, research group, and citations (full details can be found in the "Appendix"). A final screening phase was performed by excluding individual papers that were not relevant to the topic or referred to other AM processes. The documents that were finally identified, which are reviewed in the following sections, are analyzed in Fig. 1 in terms of publication trend over time (Fig. 1, top-left panel), country (Fig. 1, top-right panel), affiliation (Fig. 1, bottom-left panel), and type of sensors used for in-line data collection (Fig. 1, bottom-right panel).

Overall, 61 papers have been identified and analyzed. First seminal studies date back to 2012–2013, 10 years after the first Arcam system was sold. To the best of authors' knowledge, before 2012 in situ sensing in PBF-EB was used only in one research study to capture the powder spreading effect during smoking events [16]. Since then, the number of publications has continuously grown, with more than 50% of studies published in the last 4 years. Most of the research has been carried out by groups located in the United States, Germany, and United Kingdom. Figure 1 shows that less than ten research groups worldwide have been active so far in this field, with at least three papers published on the topic. Figure 1 also shows that most of the literature has focused

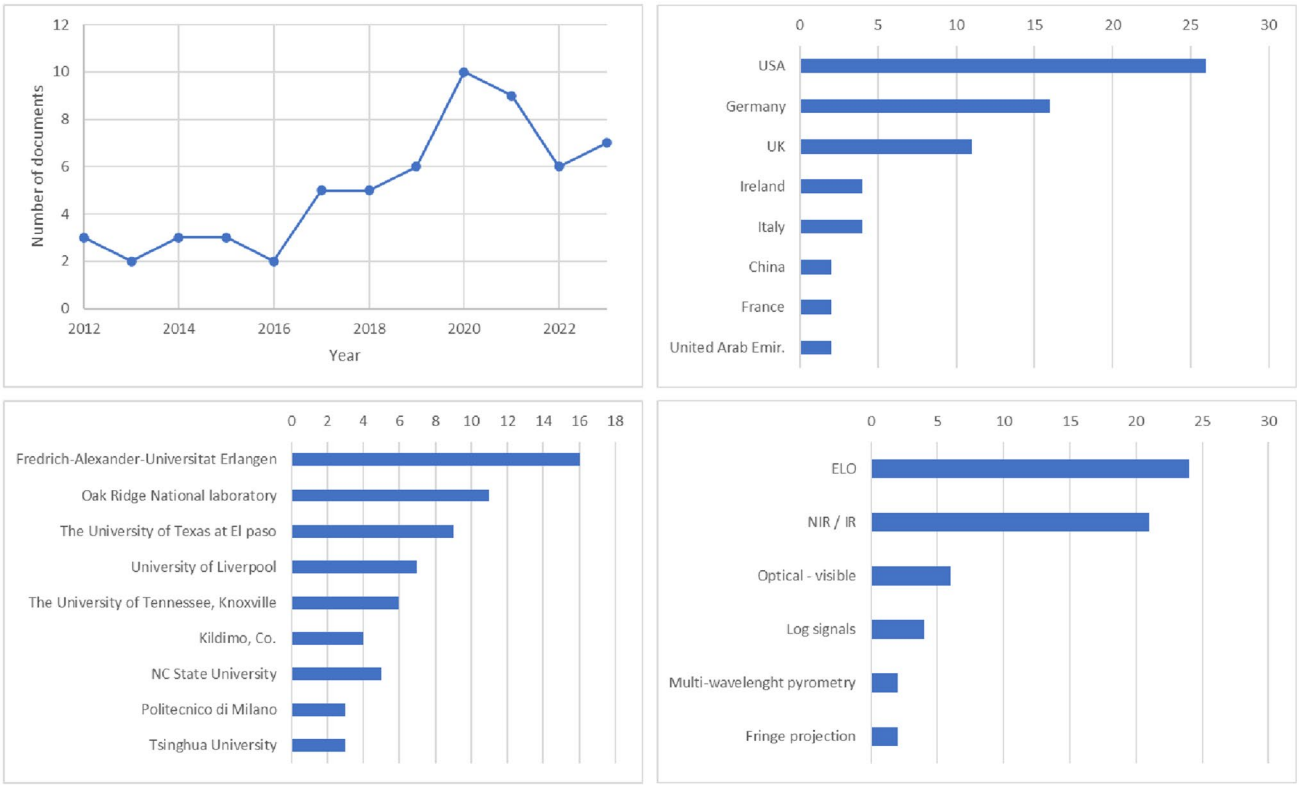

Fig. 1 PBF-EB literature on in-situ sensing and monitoring based on Scopus and Google Scholar databases: trend over time of the number of papers (top-left panel), country of the authors (top-right panel), affiliation of the authors (bottom-left panel), and type of sensor used for in-situ data collection (bottom-right panel)

on two sensing methods only, namely electron optical imaging, also known as ELO, and near infrared (NIR) or infrared (IR) video imaging. ELO consists of layerwise intensity maps generated by converting the detection of low-energy secondary electrons (SE) and high-energy back scattered electrons (BSE) as by-products of the interaction between the electron beam and the material into a current signal, then represented as a spatial map within the area scanned by the electron beam [1–5, 48]. Since the intensity of SE and BSE depends on the atomic number of the specimen and surface topography, ELO can be used to generate a spatially resolved map of the powder bed, which allows one to characterize the solidified layer in terms of surface pattern and geometry. NIR and IR video imaging methods have been widely used in PBF-EB too [6, 8, 12, 46, 47, 70], as they are suitable to capture thermal inhomogeneities or anomalous temperature distributions that may be drivers of defects. Moreover, they enable the analysis of spatio-temporal temperature (or irradiance) gradients as proxies of the final microstructural properties of the part [6] and the cited literature therein).

Additional sensing methods proposed and tested in other studies include optical video imaging in the visible range, either with high-spatial or high-temporal resolution, the use of log signals as sources of information for in-line detection of defects and anomalies, spatially integrated pyrometry exploiting multi-wavelength sensors for local temperature measurement, and fringe projection combined with cameras equipped with sensors in the visible range for surface topography reconstruction. All these methods as well as the data analytics techniques proposed in the literature for process monitoring, classification, and quality prediction are reviewed and discussed in the following sections.

3 On-the difference between in situ sensing and monitoring in PBF-EB and PBF-L

Equipping PBF-EB systems with sensors for in situ monitoring raises various challenges related both to the use of an electron beam as energy source and to the temperature and vacuum conditions involved in the process. These challenges are among the reasons behind the reduced number of studies on in situ sensing and monitoring devoted PBF-EB compared to the ones to PBF-L. One major challenge regards the need to protect any viewport from X-ray emissions generated during the beam—material interaction, and from the metallisation caused by the vaporization of alloy elements under high vacuum conditions. One possible approach to protect

viewports and sensors consists of using a mechanical shutter, which is kept closed during the heating and melting steps, and opened only when the electron beam is turned off. This approach is the one used by the LayerQam™ system, namely the NIR powder bed camera embedded in some PBF-EB systems developed by Arcam. A mechanical shutter protection has been used in some other studies too [52]. This approach limits in-line data acquisition to powder bed imaging only, preventing any data acquisition during the melting step.

Another common approach consists of equipping viewports with a leaded glass for X-ray protection and a rolling Kapton film to prevent metal vapour from adhering to the window. The main limitation of this approach consists of the severe attenuation of the signal. Indeed, the Kapton film has an IR transmission of about 79%, whereas a 10 mm thick leaded glass window has an IR transmission of 1.08% [14].

Moreover, depending on the specific machine configuration, heat shields are used to preserve the temperature distribution within the chamber and to collect the metal vapour deposition on sacrificial plates. When present, they impose additional limitations in terms of available fields-of-view and view angles for in situ monitoring sensors.

Some examples of in situ sensing setups in PBF-EB are shown in Fig. 2.

The need to screen X-ray emissions and material metallisation, together with the high temperature kept within the build chamber, also make sensor installation inside the chamber more difficult than in PBF-L. Examples of sensing methods that involve a device installation inside the chamber include air-borne acoustic emission sensors and blade-mounted sensors for high-resolution measurement and characterization of the powder bed [23] and the reviewed literature therein). These methods are hardly applicable in PBF-EB, and no attempt to adapt similar approaches from PBF-L to PBF-EB has been carried out so far.

Another difference between the two processes regards powder bed imaging in the visible range, which is the most commonly available sensing method currently embedded in industrial PBF-L machines. An example to clarify such difference is shown in Fig. 3 [21], where the top panels show two powder bed images acquired just after powder recoating with an off-axially mounted camera in the visible range in PBF-L (Fig. 3a) and in PBF-EB (Fig. 3b). Figure 3a depicts a typical example of a post-recoating image showing a homogeneous powder bed in PBF-L. Also the PBF-EB powder bed shown in Fig. 3b was spread homogeneously, but the nature of the image is quite different. Bright areas correspond to the hotter regions of the previously melted layer, which are still visible through the newly deposited layer of cold powder. This makes the assessment of the powder bed homogeneity much more challenging than in PBF-L. Another example is shown in Fig. 3, bottom panels. Figure 3c shows an example of solidified layer in PBF-L captured with a standard powder bed camera, while Fig. 3d shows an example of solidified layer in PBF-EB captured with a LayerQam™ on an Arcam machine. The two images

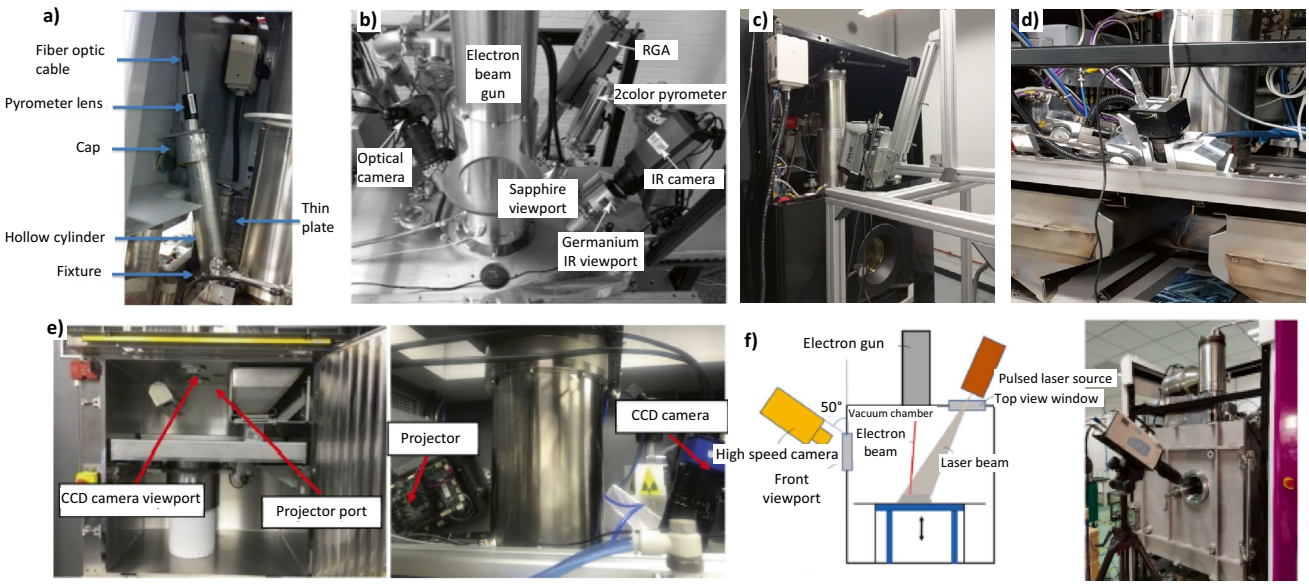

Fig. 2 Examples of video imaging setups in PBF-EB: **a** Off-axis pyrometer installed on the top viewport of an Arcam S12 system, [11], **b** multi-sensor setup on a customized Arcam A2 system including an optical camera, a 2 color pyrometer and an IR camera, [29], **c** high-speed thermal camera that exploits the top viewport of an Arcam A2 system; **d** high-speed camera in the visible range that exploits the top viewport of an Arcam A2 system [24], **e** prototype in-situ fringe projection setup composed by a projector and a CCD camera, [32, 33], **f** high-speed video imaging from the front chamber viewport of a QbeamLab 200 from QuickBeam Tech. Co, Ltd., [60]

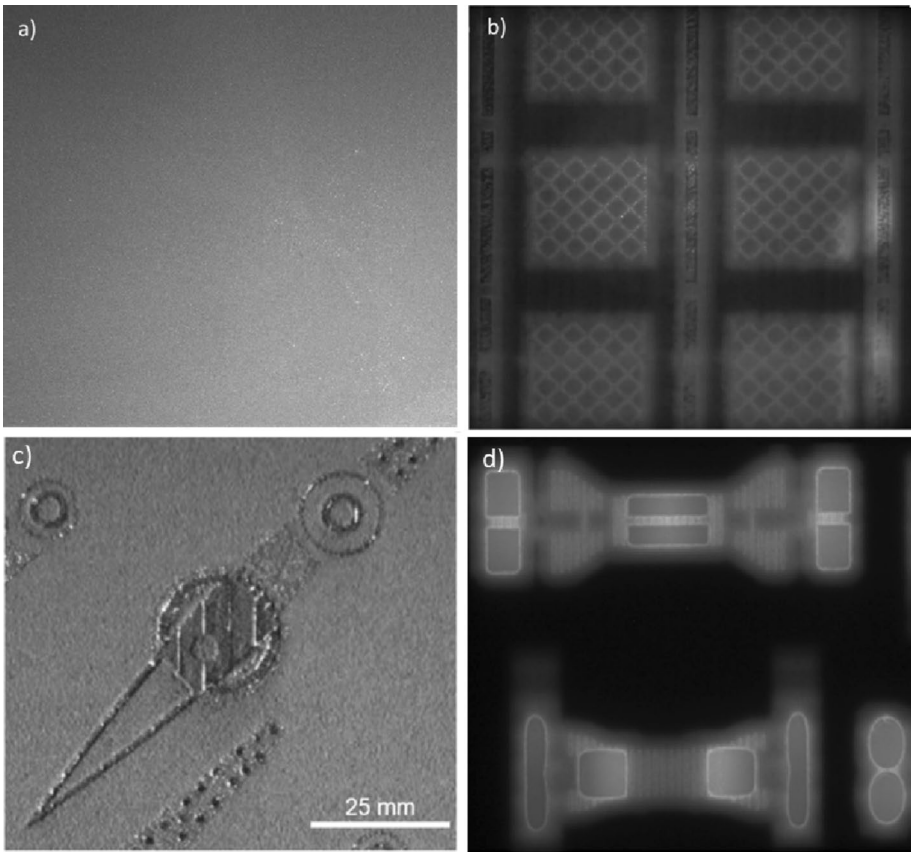

Fig. 3 Examples of post-spreading powder bed images in PBF-L (**a**) and PBF-EB (**b**) [21], examples of post-melting powder bed images in PBF-L (**c**) [42] and PBF-EB (**d**) [69], both post-spreading and post-melting images in PBF-EB (right panels exhibit a pixel intensity pattern that is influenced by the very high temperature of melted areas and their surroundings as well as high temperature gradients within the build area

were acquired with comparable spatial resolution, but the much higher temperature in PBF-EB has a detrimental effect on the quality of the image (blur halo around the solidified layer, pixel intensity variations induced by the surface temperature, etc.).

Despite the above-mentioned limitations, PBF-EB also opens to some sensing opportunity that is not available in PBF-L. Indeed, the interaction between the electron beam and the material generates by-product emissions that can be effectively used for process monitoring purposes, namely X-ray, SE, and BSE emissions. In-line X-ray measurement has been limited so far to the beam calibration task only, while SE and BSE detection is at the basis of the ELO imaging technique [1, 2, 4, 63], which currently represents the major stream of research on in situ sensing and monitoring of the PBF-EB process, as shown in Sect. 2. ELO has the advantage of requiring no viewport and no protection from X-rays and metal vapour deposition (more details are provided in Sect. 4), and hence, it represents a well-suited approach for the PBF-EB process, as it exploits the intrinsic features of the process while avoiding the limitations that affect alternative methods.

One latter difference between in situ sensing and monitoring methods in PBF-L and PBF-EB regards the capability to measure the salient properties of the melt pool. In PBF-L, melt pool monitoring via co-axial sensors, either spatially integrated (e.g., photodiodes) or spatially resolved (high-speed cameras) is one of most investigated methods for in-line detection of process instabilities and defects [23, 35]. The co-axial measurement is enabled using the same optical path of the laser. In PBF-EB, a similar co-axial sensing approach is not possible. Melt pool imaging and monitoring in PBF-EB has been explored only in a few studies using off-axially installed sensors [31, 53, 54], but the limitations in terms of both temporal and spatial resolution over the whole build area make this approach hardly application for industrial use.

An in-depth discussion of in situ sensing and monitoring methods that have been proposed so far for the PBF-EB process is presented in the next Section.

4 In situ sensing and monitoring methods in PBF-EB

In Grasso et al. [23], a classification of in situ sensing and monitoring methods in PBF was proposed, based on five different levels at which in situ data could be gathered and used. Level 0 refers to the use of so-called log signals, i.e., signals acquired through embedded machine sensors (e.g., chamber and column pressure, beam current and voltage, grid current, pulse signals, etc.) with no need for external

sensors. Level 1 refers to 2D or 3D measurements of the powder bed, either before or after the powder deposition, to characterize the power bed homogeneity or the solidified layer geometry and topography. Level 2 refers to measurements gathered during the melting operation, aiming to capture the salient dynamics of the interaction between the electron beam and the material, and the associated heating and cooling patterns. Level 3 refers to the measurement of the salient properties of the melt pool, in terms of size, shape, temperature profile and stability over time. Level 4 finally refers to measurements that allows to determine phenomena and process dynamics occurring under the currently processed layer. This same classification is adopted in this study to divide the literature into different research areas. The result of such classification is shown in Table 1, where the literature is further classified also in terms of the measured quantities, referred to as "signatures", and the sensing method.

4.1 Process monitoring via log-signals (level 0)

Log-signals were pointed out to be correlated with process errors and undesired variations of the process conditions [56]. Indeed, they are commonly used in PBF-EB for post-process diagnostics. However, the high number of signals imposes the use of appropriate approaches for data visualization and analysis. The data visualization tool developed by Steed et al. [56] was used in some studies to investigate correlations between log signals and actual defects in parts [69]. Ledford et al. [30] used some log-signals like the beam speed, the electron gun filament current feedback, and the column pressure to generate 3D data maps across multiple layers and areas of interest. Such maps could reveal local discontinuities that may be the root cause of anomalies and defects, and hence they can be used as in-line sources of information for process monitoring. Chandrasekar et al. [10] studies the rake position and rake sensor pulse signals to gather information about the powder spreadability, aiding the detection of powder deposition errors. Grasso et al. [22] investigated the use of rake pulse sensor signals to develop a machine learning tool for the automated detection of defects related to incorrect powder spreading conditions. The proposed approach allowed the anticipated detection of geometrical distortions caused by powder recoating errors. These seminal studies open to a variety of possible uses of log-signals in the framework of in situ process monitoring. However, the wide natural variability of the these signals and the limited sampling frequency adopted in industrial

Table 1 Classification of the literature on in situ sensing and monitoring depending on the monitoring level, the measured quantity (signature) of interest, and the sensing method

Signatures of interest	Sensing method	References (PBF-EB)
Level 0		
Log-signals	No external sensor	[10, 22, 30, 56, 69]
Level 1		
Surface pattern or height map of the powder bed	Off-axis imaging in visible range	[23, 24]
	Fringe projection (with single or multiple off-axis cameras)	[32–34]
Surface pattern or height map of the printed slice	ELO	[3, 5, 7, 9, 28, 29, 30, 43, 48, 63, 66, 67, 71]
	Off-axis NIR/IR imaging	[12, 37, 38, 40, 50, 51, 55, 69, 70]
	Fringe projection (with single or multiple off-axis cameras)	[32, 34]
Geometrical accuracy of the printed slice	ELO	[1, 2, 4, 61, 64–67]
	Off-axis NIR/IR imaging	[37, 38, 50]
Solidified layer material composition	ELO	[63]
Level 2		
Heatmap/heating and cooling profiles	Off-axis video imaging in the visible range	[24, 31]
	Off-axis NIR/IR video imaging	[6, 8, 11, 14, 18, 20, 26, 29, 31, 39, 44–47, 52]
	Off-axis spatially integrated pyrometry	Terrazas-Najera et al. [58] [11, 17, 29]
Smoking events	ELO	[68]
	Off-axis video imaging in the visible range	[16, 60, 68]
Level 3		
Melt pool size and shape	Off-axis video imaging in the visible or NIR range	[31, 53, 54]
Level 4		
Melt pool penetration and phase transition	X-ray video imaging	[15]

machines currently limit the probability to detect actual defects, while inflating the risk for false alarms. So far, there is a lack of studies that quantitatively investigate the power of log signal-based monitoring techniques in terms of false positive and false negative rates. Nevertheless, their potential for automated process monitoring has been not fully explored, and future research developments may be seen in the future.

4.2 Powder bed monitoring (level 1)

Level 1 methods for powder bed imaging and monitoring have attracted a quite large interest in the literature. In this case, it is possible to distinguish between two major aims. The former consists of determining errors and discontinuities in the powder deposition, possibly caused by a damage recoater, powder dosing errors, superelevated edges, or surface contaminations. The latter regards the characterization of the solidified layer, either in terms of its geometrical deviations from the nominal, or in terms of its surface topography. A widely investigated layerwise measurement and monitoring approach is the one based on the ELO methodology. The underlying idea consists of converting SEs and high-energy BSEs into a current signal. The 1D signal is then mapped into a 2D image by linkining its value to the synchronous electron beam location, analogously to what is done in scanning electron microscopy. The detection of SEs and BSEs is made possible by using simple detectors inside the chamber or between the chamber and the electron gun [a few possible experimental setups are shown in Fig. 4, including both single detector (a–c) and multi-detector methods (d)].

Although the ELO approach avoids most issues and limitations that affect standard video imaging methods, the natural features of the PBF-EB process introduce some challenges in this case too. Indeed, the working principle of BSE detectors is affected by high temperatures, while metal vapour deposition on the the detectors may interfere with the measurement. Wong [62] also showed that there is an helium gas amplification effect on the ELO image quality and contrast. Because of these issues, various ELO configurations have been proposed in the literature, to enhance the quality of the data and to make the system robust to nuisance factors.

A primary use of this approach involved the layerwise reconstruction of the surface pattern of the solidified layer, as a proxy on non-optimal melting conditions and internal porosity. Arnold et al. [5] used ELO to capture post-hatching ELO images. In situ detected irregularities of the solidified surface induced by varying the beam power in the melting phase were shown to be well representative of part porosity structures observed via post-process optical microscopy and X-ray computed tomography (CT) (Fig. 5a). Similar results were obtained in PBF-EB of pure copper by Ledford et al.

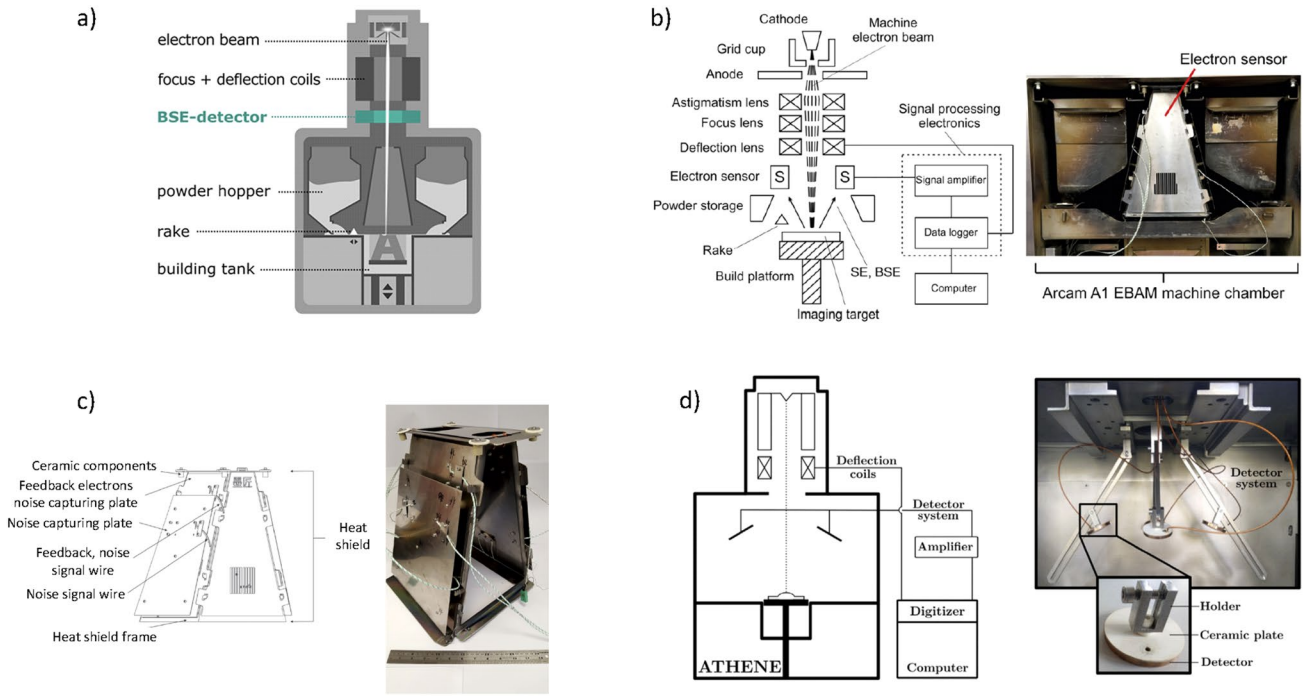

Fig. 4 Examples of in-situ sensing setups for ELO imaging: **a** setup with BSE detector under the focus and deflection coils, [5], **b** prototype setup where heat shield plates are used as detectors, [66] detail of the heat shield adaptation to backscattered electron detection, [67]) example of the multi-detector system in [48]

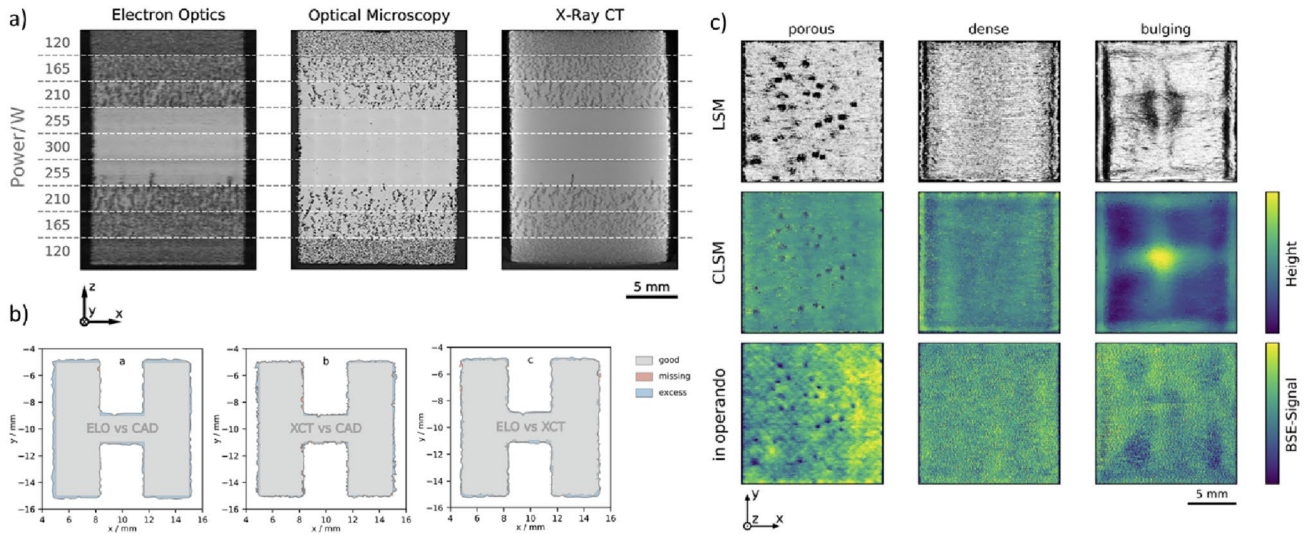

Fig. 5 Examples of ELO imaging in PBF-EB: **a** comparison between in situ detected pores via ELO and ground-truths based on optical microscopy and X-ray CT [5], **b** example of ELO used to estimate the deviation from the nominal geometry and from the X-ray CT-based ground truth, where both the presence of missing material and excess of material are presented, highlighting the good geometrical agreement with respect to the reference [1], **c** example of in-operando ELO maps compared with ground truth, where LSM stands for laser scanning microscopy, and CLSM stands for confocal laser scanning microscopy [3]

[30]. Ledford et al. [29] showed that ELO images could capture pores generated in overhang regions during the production of pure copper. Le Roux et al. [28] compared different convolutional neural networks (CNN) to classify ELO images of parts produced with different process parameters into different categories, namely good, porous and bulging. Classification accuracy of about 95% was achieved with respect to true categories defined via manual labelling. Bäreis et al. [7] showed that ELO could also be used for the in situ detection of cracks in the soldified layer during the PBF-EB of a nickel-based superalloy such as CMSX-4.

As pointed out by Pobel et al. [43], the correlation between the surface pattern of the solidified layer measured via ELO and the final part porosity may be used for in-line process optimization, i.e., for the identification of the printability window using in situ gathered ELO images in place of post-process destructive or non-destructive inspections. Breuning et al. [9] leveraged on this possibility in their study of a process optimization approach for complex shapes based on the introduction of a characteristic scan length-dependent process parameter limit. ELO images were used to characterize the resulting surface morphology induced by different scan length-related process conditions.

Another stream of research on the use of ELO in PBF-EB regards the in situ estimation of geometrical accuracy and geometrical/dimensional deviation from the nominal (Fig. 5b shows an example of example of geometrical deviation between the in situ reconstruction based on ELO imaging, the nominal geometry, and the X-ray CT-based ground truth). Arnold and Körner [1, 2] showed that the average local deviation between in situ ELO-based and post-process X-ray CT-based geometry reconstructions was below 100 µm, whereas the maximum local deviation was in the order of magnitude of the surface roughness. Arnold and Körner [1, 2] pointed out the relevance of post-processing operations on ELO images to deal with the accuracy of beam deflection and data registration, and to keep into account the thermal shrinkage of the part. Grounding on these results, Arnold et al. [4] showed that combining post-process X-ray CT measurements with in situ ELO imaging and thermodynamic simulation could enable an in-depth characterization of the inherent PBF-EB accuracy and thermally induced distortions.

Despite benefits and potentials of the ELO methodology, its basic implementation involves an additional step for image acquisition, since the electron beam scanning of the layer is needed for measurement purposes. This issue has been overcome in more recent studies that proposed a so-called "in-operando" BSE detection, i.e., directly during the melting stage. This approach was first presented in Arnold et al. [3]. Figure 5c shows an example from Arnold et al. [3] where the in situ measurement is compared against two ground truth references, one based on laser scanning microscopy (LSM), and one based on confocal laser scanning microscopy (CLSM). The 2D signal intensity map gathered during the melting stage was pointed out to be well correlated to the final topography of the layer measured with other benchmark methods. The "in-operando" ELO measurement was compared to co-axial spatially integrated measurements of the melt pool in PBF-L, where 1D photodiode signals are

usually represented in terms of 2D intensity maps. However, rather than providing information about the salient properties of the melt pool, the in-operado ELO image contrast is mainly dominated by the way in which the surface topography affects the BSE emissions, and hence the resulting intensity map can be used as a proxy of the surface pattern of the scanned area.

Generally speaking, the resolution of the ELO imaging technique depends on the scan line distance, the beam diameter, the scan speed and the sampling rate of the measuring device [3]. The spatial resolution achieved in most stdies ranges between 50 and 100 µm/pixel. As an example, Arnold et al. [5] obtained a pixel resolution of 60 µm/px, exploiting a raster scanning of the surface with a beam diameter of about 300 mm, an exposure time of 0.1 ms/px and a beam current to 7 mA. Such resolution is higher than the one commonly available with industrial powder bed cameras in PBF-L, but also higher than spatial resolutions made available with most optical imaging methods in PBF-EB [23].

More recently, multi-detector ELO imaging has been proposed too. Similarily to stereo imaging, the combination of multiple BSE detectors allows one a three-dimensional determination of target locations in space. When properly calibrated, such measurment system enables the reconstruction of a height map of the layer. In SEM, the sum of signals from opposite detectors is sensitive to material composition, whereas their difference is sensitive to the actual height map of the sample. Levering on this, multi-detector ELO has been proposed by Renner et al. [48] and Zhao and Lin [71]. In Renner et al. [48], four detectors were used to gather four different viewing directions to compute local surface gradients, generate a high-resolution heigh map of the layer, and precisely locate ridges and grooves in bulging surfaces. As shown in Fig. 6, the recostructed topography of test samples was compared against a ground truth based on LSM. Figure 6a shows a rendering of the ground truth surfaces measurement, while Fig. 6b shows a rendering of the in situ reconstructed height map of the same surface. The resulting profiles were in good agreement, with a mean different of 32 µm (Fig. 6c). To the same aim, a dual detector were proposed in Zhao and Lin [71], who also showed the linear correlation between the electronic current and surface height gradient.

Renner et al. [49] presented a simulation model suitable to determine the effect of the detector position on the resulting image contrast and quality. It can be used as a predictive method for the optimal design of ELO detectors and to compute build surface height gradients with no need for calibration operations.

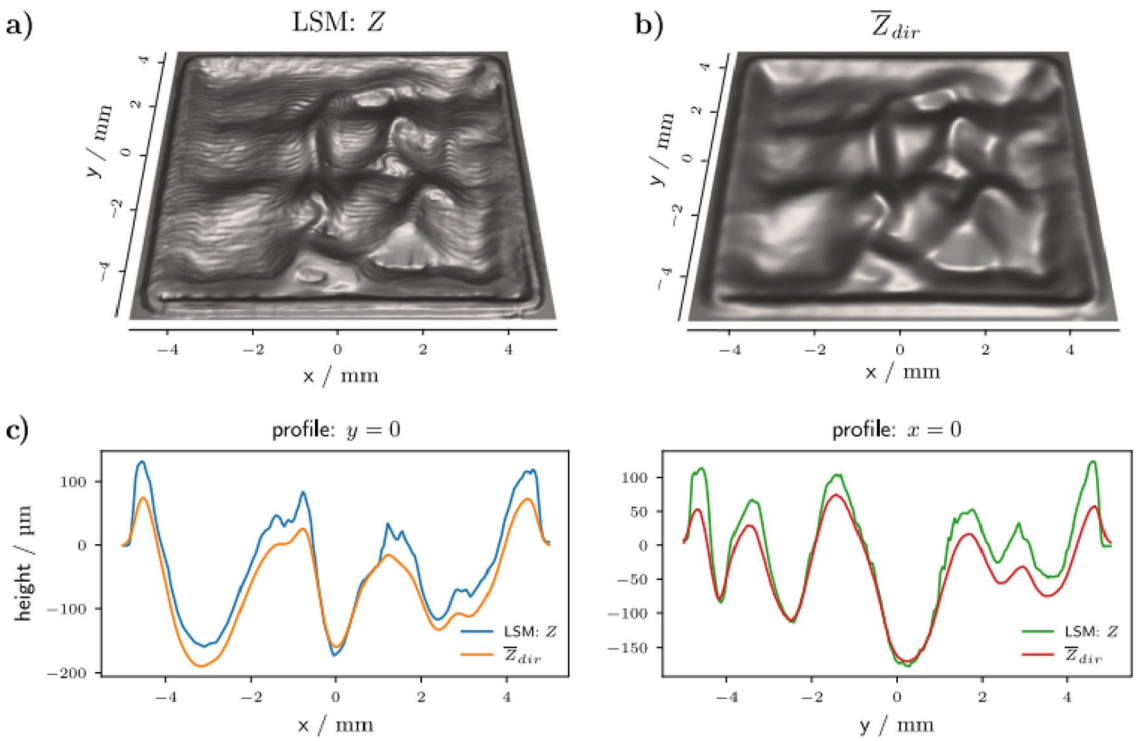

Fig. 6 Examples of in-situ height map reconstruction of the solidified layer via multi-detector ELO and comparison against a ground truth measurement based on LSM stands for laser scanning microscopy (LSM): **a** rendering of the LSM measurement, **b** rendering of the in-situ reconstructed surface, **c** comparison of height profiles along the y direction, $y = 0$, **d** comparing of height profiles along the x direction, $x = 0$ [48]

An alternative method for the in situ reconstruction of the height map of the layer was proposed by Liu et al. [32–34], based on fringe projection combined with optical imaging.

The use of fringe projection in PBF-EB on commercial machines from Weyland Precision was investigated by Liu et al. [32, 34]. The proposed system involved a single-view architecture, composed by a structured light projector and a camera. The fringe projection measurements were taken during the time window between powder recoating and fusion and after EB melting. The measurement time was about 2 s during each measurement cycle, with an absolute error with respect to benchmark interferometer measurements between 2 and 7 µm. The system has been fully deployed on a commercial machine and it is currently implemented on PBF-EB systems developed by Wayland Additive.

A method for the automated detection of powder spread errors was proposed by Grasso [21], where a high-spatial resolution camera and no additional illumination source was used on an industrial system. Grasso [21] presented an automated powder bed monitoring methodology that allowed to combine pre- and post-recoating images to automatically identify regions of the powder bed where either an excess or a lack of powder was present. Since the new powder layer is colder than the underneath layer, an excess of powder results into a darker spot (or region) in the fused image, while a lack of powder results in a brighted spot. The method was shown to be effective in detecting powder bed inhomogeneities that caused internal lack-of-fusion defects as well as geometrical distortions. An example is shown in Fig. 7a, where the left panel shows the transfer function used to isolate low-intensity and high-intensity regions of interest, whereas the right panel shows the automatically detected anomalies in the powder spreading (red areas). The spatial resolution was 130 µm/pixel over a 210 × 210 mm build area.

Rather than monitoring the homogeneity of the powder bed, optical imaging in the NIR range is commonly used in PBF-EB to detect irregularities in the solidified layer. This approach is commercially available on Arcam machines. Some authors showed that local pixel intensity variations as well as the bright spots within the solidified area can be proxies of volumetric flaws and distortions in the part [40, 69, 70]. Yoder et al. [70] showed that pores could be identified simply by setting a threshold on the pixel intensity, because bright spots were assumed to be caused by surface cavities. Depite a qualitative correspondence between pore concentrations in post-process X-ray CT measurements and in situ detected bright spots has been shown in various studies, there is still a lack of a rigorous performance assessments in terms of false positive and false negative rates, and probability-of-detection functions. A similar approach was investigated in more depth in Croset et al. [12]. Croset et al. [12] showed that NIR layerwise imaging in PBF-EB can be used to detect wrong sets of process parameters not only in terms of volumetric defects, but also in terms of geometrical deviations from the nominal. In particular, an over-melting condition was shown to produce a significant increase of the deviation with respect to normal melting. An example of NIR images of the powder bed acquired in different process conditions is shown in Fig. 7b, together with the corresponding post-process optical images [12]. In this case, the spatial resolution was 75 µm/pixel over a 210 × 210 mm build area.

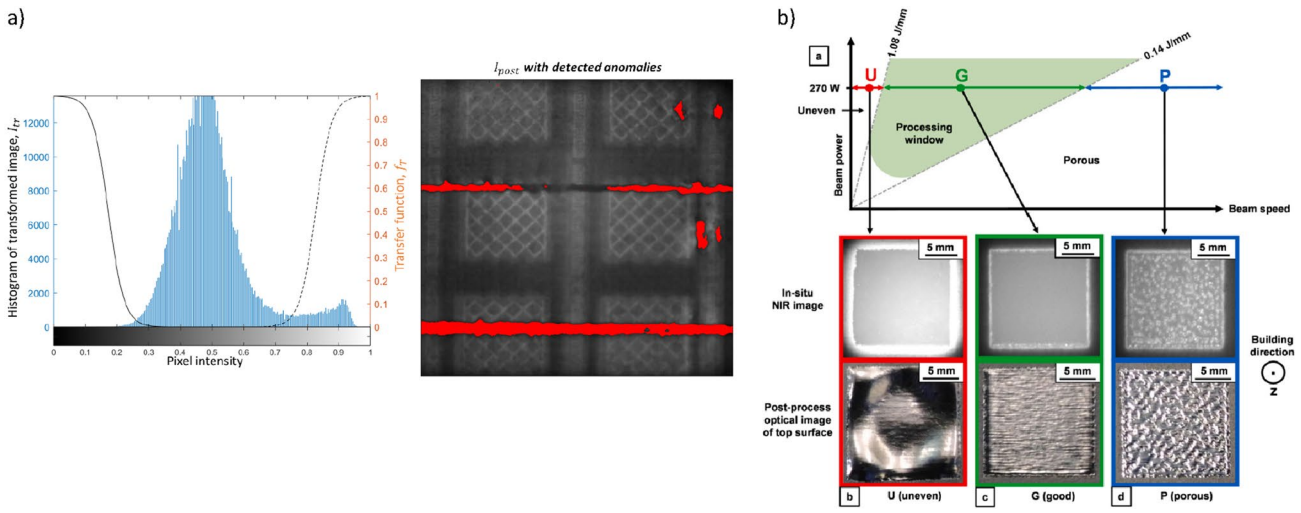

Fig. 7 **a** Examples on the use of optical imaging for powder bed homogeneity monitoring: left panel shows the transfer function used to isolate low-intensity and high-intensity regions of interest; right panel shows the automatically detected anomalies in the powder spreading (red areas) [21], **b** Example of the use of NIR imaging to classify process conditions—a comparison between in situ NIR images of the solidified surfaces and post-process optical images of the same surfaces for different energy density levels [12]

4.3 Monitoring of process dynamics during layer melting and cooling (level 2)

NIR and IR video imaging has been used since the first seminal works on in situ monitoring in PBF-EB to capture the local and global heating and cooling patterns in every layer, either for the detection of volumetric defects or for the prediction of final microstructural properties. The latter problem in particular, attracted an important stream of research ([13] and references therein). Being able to predict microstructural properties in-line, such as grain size and orientation, allows detecting deviations from a target microstructure and enables the development of functionally graded products. The seminal study of Raplee et al. [47] showed the feasibility of in situ thermography to estimate a spatial map of thermal gradients (G) and solid–liquid interface velocities (R), which were then used to distinguish regions characterized by either columnar grains or equiaxed grains obtained by varying the scan strategy from line scan to point-wise scan. Figure 8 shows an example of in situ thermal map of a layer after IR image calibration, the histogram of the G/R ratios estimated in situ for the two scan strategies [46, 47], and a sample functionally graded bracket built by locally varying the scan strategy [6]. Following studies further demonstrated the feasibility of in situ site-specific microstructure control, mainly for nickel-based superalloys. However, a certain amount of uncertainty was pointed out in the prediction of the final microstructural properties [6], and possible improvements may be envisaged in future research.

IR thermography has been used in the literature for thermal gradient analysis using sensors sensitive to either long or medium wavelength radiation. Cordero et al. [11], Rodriguez et al. [52], Mireles et al. [37, 38] used long wavelength IR cameras, with a spatial resolution between 175 and 350 µm/pixel. Raplee et al. [47] and Babu et al. [6] used a medium wavelength IR vision, with a higher spatial resolution in the order of 35 µm/pixel. Temporal resolutions where limited in all mentioned studies, in the order of ten frames per second. Despite the attenuation caused by the Kapton film and the leadglass protection, in situ IR video imaging was demonstrated to be suitable to measure local gradients and detect changes and variations connected with process anomalies.

Apart from in situ microstructure prediction, Babu et al. [6] showed that spatial IR maps could reveal also cracking patterns across different layers during the PBF-EB of nickel superalloys. Boone et al. [8] instead, adopted a NIR vision setup equipped with a custom designed borescope lens system. The use of a NIR camera was motivated by the much higher transmission of the leadglass and Kapton film protections in the NIR range (about 76%) compared to the one in the IR range. Boone et al. [8] showed an exprimental study where spatial NIR intensity maps were used to detect geometrical distortions and swelling defects in overhange regions caused by an anomalous heat accumulation. Figure 9a shows the test specimen adopted in Boone et al. [8]. Figure 9b shows an example of the thermal map showing both lack of fusion defects (small localized apparent hot-spots) and swelling defects (indicated with maker). Figure 9c shows the manufactured part where the actual swelling is highlighted.

An issue of primary importance for in situ measurement of absolute temperatures regards the thermal image calibration. The target emissivity shall be known to convert the raw image (where pixel intensities correspond to the measured irradiance) into an actual temperature map. However, the local and instantaneous emissivity estimate is made difficult, or even impossible, by fast phase transitions from powder to liquid and from liquid to solidified material, continuous changes in surface properties, and emissions of metal vapour. One simple approach consists of applying a conversion factor such that the temperature

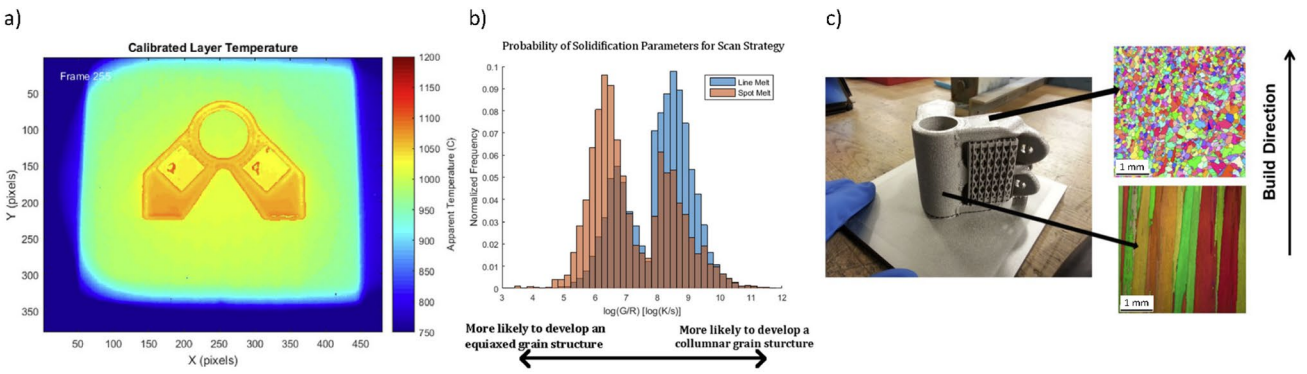

Fig. 8 Examples from Raplee et al. [47] and Babu et al. [6]: **a** in situ thermal map of a layer after calibration, **b** histogram of the G/R ratios estimated in-situ for the line and point (spot) scan strategies, **c** completed PBF-EB alloy 718 bracket built with equiaxed grain formation in the spot melt region and columnar grain formation in the raster melt region

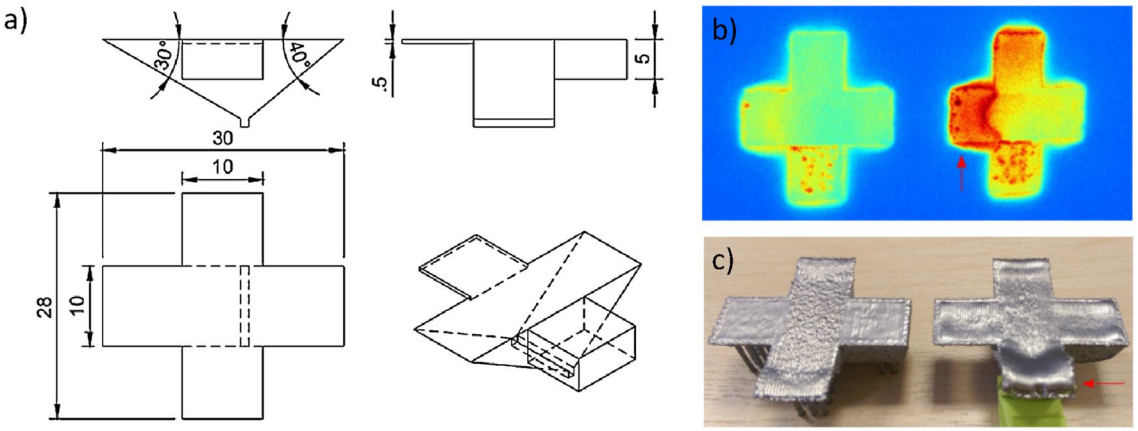

Fig. 9 **a** Example of in-situ NIR video imaging for the detection of a swelling distortion: **a** sample part (dimensions in mm), **b** thermal map showing lack of fusion defects (small localized apparent hot-spots) and swelling (indicated with maker), **c** manufactured part showing evidence of swelling (indicated with marker) [8]

measured within the melt pool region corresponds to the known liquid–solid transition temperature of the material. However, this is not accurate enough for estimates of thermal gradients needed for in-line microstructure prediction. A more rigorous approach involves a calibration procedure where the temperature of a test sample is measured by both thermal cameras and embedded thermo-couples [52].

Two-color pyrometry and IR video imaging has been proposed by some authors to ease absolute temperature measurements (the reader is referred to the studies reviewed in [23]). However, Fernandez et al. [17] showed that the emissivity of the material may exhibit consistent spectral and temporal dependences which make accurate temperature measurements quite challenging. To this aim, Fernandez et al. [17] used an in situ measurement setup based on a multi-wavelength pyrometer suitable to resolve hundreds of wavebands of amplitude 2 nm in the spectral range 1000–1650 nm. The pyrometer was mounted with a fixed measurement spot within the build area. Terrazas-Nájera et al. [58] used the same setup to measure the signal strength as proxy of the material emissivity during all PBF-EB process stages. Terrazas-Nájera et al. [58] showed that the proposed approach was sensitive enough to detect the dynamic thermal signal strength/emissive transitions of materials associated with surface temperatures, phase transitions, chemistry and powder morphology variations from layer to layer and from build to build.

Video imaging in the visible range at high temporal resolution was proposed by Grasso et al. [24] as an alternative approach to IR vision. Indeed, thermal cameras are more difficult to install on industrial machines, especially when high spatial and temporal resolution is needed. Grasso et al. [24] presented a study on the detection of local over-heating phenomena known as "hot-spots", i.e., locally over-heated areas where a diminished heat exchange with the surrounding material may lead to micro- and macro-geometrical distortions as well as volumetric defects and discontinuities. Since regions affected by hot-spots stay hot for a longer time with a slower cooling drift than in normal conditions, they can be detected as anomalous bright spots in the visible range too. Figure 10a shows an example from Grasso et al. [24] where hot-spots are visible as local peaks in the 3D map of the proposed synthetic index designed to capture anomalous heat accumulations.

High-speed vision in the visible range was also used by other authors for different purposes. Lee et al. [31] used it to monitor the dynamics of so-called "ghost beam" during the development of novel scan strategies. Wang et al. [60], Ye et al. [68] and Eschey et al. [16] used high-speed vision to study the smoking phenomenon, which is relevant to prevent it or, at least, to anticipate its detection and recover the process after its occurrence. Both Wang et al. [60] and Ye et al. [68] showed that the smoke phenomenon is a multi-stage event, characterized by a stable stage, followed by a meta stable powder fume development stage and finally by a catastrophic powder explosion (an example is shown in Fig. 10b). Combining high-speed video imaging with ELO imaging, Wang et al. [60] and Ye et al. [68] demonstrated the suitability of the ELO methodology to capture each development stage. Such capability makes the ELO imaging technique suitable for early detection of smoking events.

As far as level 2 monitoring methods are concerned, one major difference between PBF-L and PBF-EB is the fact that great attention has been devoted to in situ spatter monitoring and analysis in PBF-L, whereas this is an unexplored field in PBF-EB. The reason is that spatters are rare events in PBF-EB, at least under normal and stable process conditions. They mainly consist of droplet spatters, i.e., molten material ejections from the melt pool, due to the pre-sintered nature of the powder in the layer that limits hot and

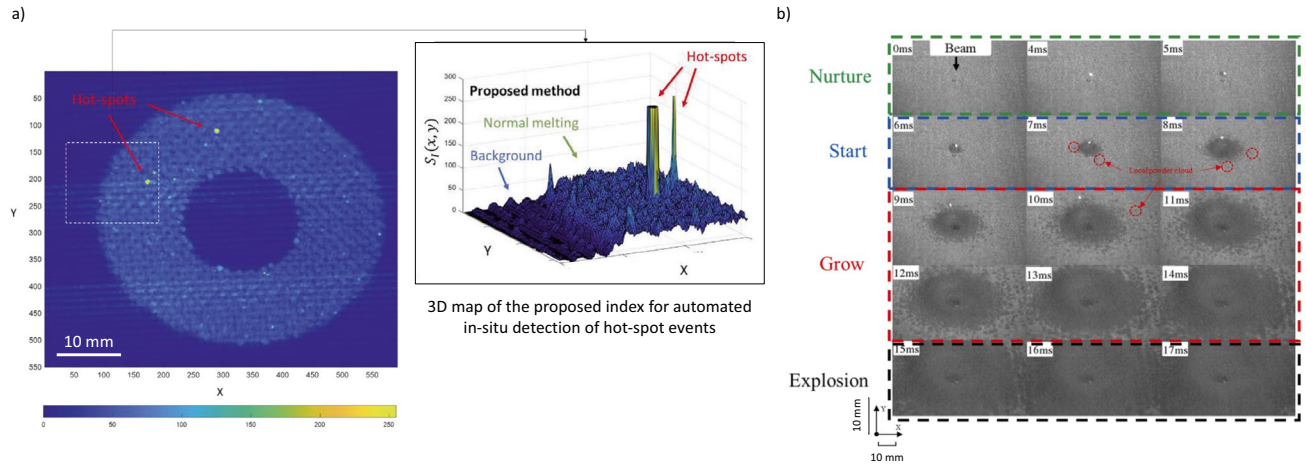

Fig. 10 **a** Example of hot-spot detection via high-speed video imaging—the peaks in the 3-D map of the proposed synthetic index indicate the presence of hot-spot events [24], **b** example of high-speed video imaging of the smoke phenomenon under the condition of fixed-position irradiation [60]

cold particle ejection phenomena observed in PBF-L. The only seminal study where spattering was captured by in situ video imaging in PBF-EB is the one of Hankwitz et al. [26], where authors showed that process conditions that produced a larger number of spatters were also responsible for a lower process quality and stability in the PBF-EB of niobium. This potentially opens to the use of spatters as proxies of unstable condition in PBF-EB as well, but additional research is needed in this direction.

4.4 Other monitoring levels

One major stream of research in PBF-L regards in situ measurement and monitoring of salient melt pool properties, as their stability over time is strictly correlated to the final quality of the product [23, 35]. The lack of any optical path for co-axial monitoring avoids the applicability of similar methods in PBF-EB. Nevertheless, a few authors explored the possibility to measure melt pool properties in restricted build locations by combining off-axis high-speed video imaging with a narrow and fixed field of view. Scharowsky et al. [53, 54] investigated the melt pool dynamics with a high-speed camera equipped with a 810 nm band-pass filter and a pulsed light source in the same wavelength. The observation area was limited to less than 10 mm × 10 mm. Frame rates of 4000 fps and 6000 fps were tested with a spatial resolution in the order of 5 µm/pixel. Scharowsky et al. [54] showed that the proposed imaging setup allows determining the aspect ratio of the melt pool in the *X*–*Y* plane. It also allows one to capture oscillations that can be attributed to the powder particle size. Examples of high-speed video image frames from Scharowsky et al. [54] are shown in Fig. 11a. In a similar way, Lee et al. [31] used high-speed video imaging to determine the melt pool geometry and intensity along scanned tracks, with an acquisition rate of 12,000 fps, showing the effect of ghost beam scan strategies on the melt pool elongation and oscillations.

One stream of research that attracted a relevant number of studies in PBF-L regards the use of ad hoc prototype machines for in situ X-ray video imaging of the melt pool penetration and its dynamics under the processed layer [23, 35]. To the best of the authors' knowledge, the only similar attempt in PBF-EB was carried out by Escano et al. [15]. An open architecture PBF-EB system was developed and tested for in situ synchrotron X-ray monitoring. High-speed video imaging in the visible range as well as high-speed IR imaging were added, too. Escano et al. [15] showed the sub-surface transient phenomena occurring during the EB melting of a Ti6Al4V powder bed. An example of in situ measurements performed in Escano et al. [15] is shown in Fig. 11b, where vapor cavities, the solidification front and sub-surface pore formations are visible. Escano et al. [15] highlighted the suitability of the proposed architecture to reveal vapor cavity and pore formation dynamics, and to capture the phase evolution thanks to in situ X-ray diffraction patterns.

The methods described in this sub-section for melt pool measurement in PBF-EB are particularly helpful to characterize the melt pool dynamics and the beam–material interactions under different processing conditions, and to investigate defect origination mechanisms. Despite not being applicable to in-line monitoring of the PBF-EB process during actual production, they are valuable research tools for process and material development and tuning. Ioannidou et al. [25] pointed out the need for more research efforts devoted to the characterization and study of the PBF-EB

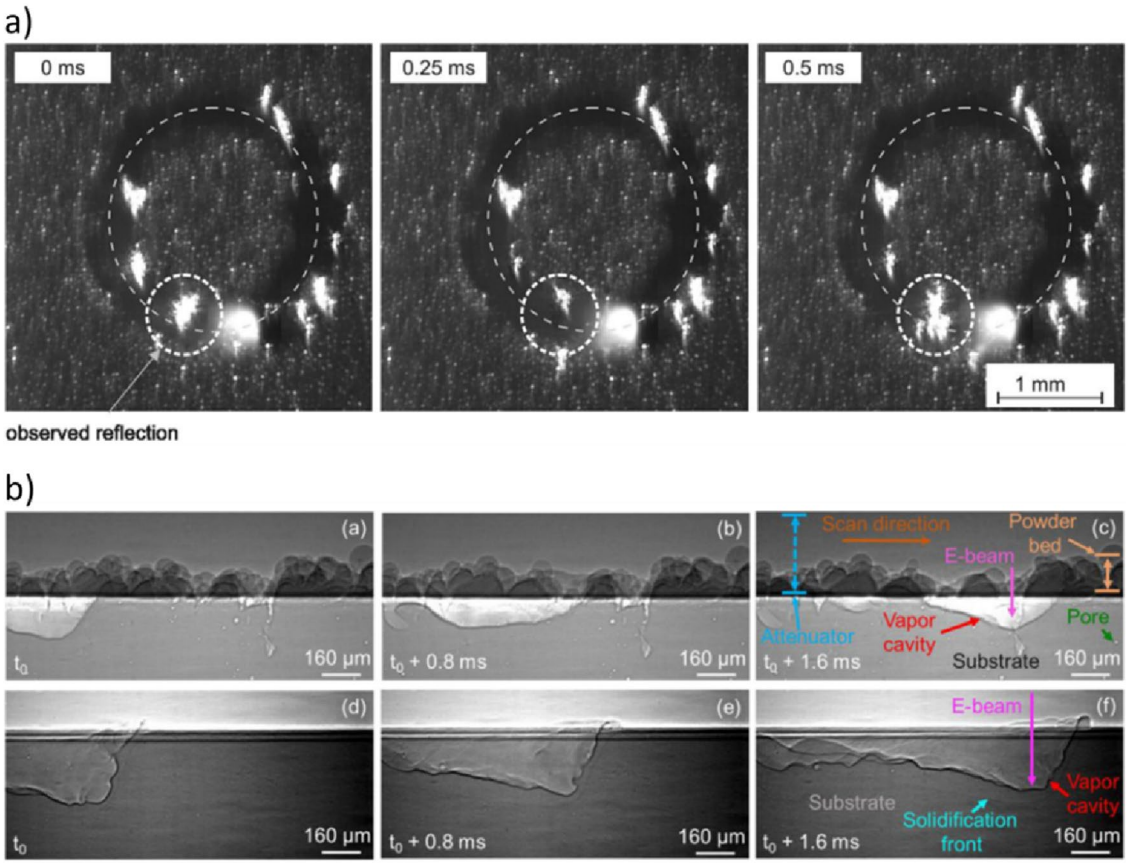

Fig. 11 **a** Example of high-speed video imaging for melt pool analysis in Scharowsky et al. [54]—the images highlight the challenging distinction between clustered reflections and the actual melt pool, **b** example of in-situ synchrotron X-ray video imaging in Escano et al. [15]—it shows the vapor cavity, the solidification front and the formation of pores on a temporal scale of few milliseconds

process via in situ synchrotron X-ray measurements. This is expected to be a field of research that may open a new comprehension of the underlying process dynamics in PBF-EB.

5 Open problems, challenges, and future perspectives

The industrial relevance of in situ monitoring of the PBF-EB process is testified by the fact that all PBF-EB machine developers have invested in equipping their systems with a variety of sensors and toolkits to this aim [19]. More specifically, Arcam provides an optical camera that captures layer images in the NIR range. Jeol provides an optical camera too, whereas ELO imaging is available on Freemelt, QuickBeam and ProBeam systems. Wayland machines, instead, are equipped with a high-speed camera and a fringe projection system for surface topography reconstruction. This variety of sensing and monitoring equipment also demonstrates that most solutions investigated in the literature are valuable for a real industrial implementation and adoption. However, there is a major gap in the literature that still needs to be filled, namely the lack of automated defect detection and/or classification algorithms. In other terms, the PBF-EB literature has focused more on the sensing problem, i.e., on measuring quantities and process signatures that correlate to anomalies and phenomena of interest, rather than on the development of monitoring solutions. Referring to the terminology defined in Grasso et al. [23], the term "in situ monitoring" refers to the capability of making sense of measured quantities to signal an alarm in the presence of an undesired process state, or to automatically classify observed patterns into normal and defective categories. Machine learning techniques have been widely investigated in PBF-L to this aim, whereas in PBF-EB they have been explored by only a few authors. Le Roux et al. [28] investigated the used of CNNs for the automated classification of ELO images into different categories, namely good, porous and bulging. A multi-class training set was used to this aim. Different CNN architectures were compares, demonstrating the capability of classifying the correct process condition simply using the ELO image of the layer. Grasso et al. [22] presented a method based

on a one-class-classification variant of Support Vector Machines (SVMs) for the automated identification of geometrical distortions caused by a wrong powder deposition in multiple layers. The method was applied to a subset of log signals, using a few copies of the monitored component as training samples. Grasso et al. [24] presented an automated hot-spot detection method based on an extension to the PBF-EB process of a method previously developed in PBF-L. The method consists of an automated pixel-wise classifier suitable to distinguish the hot-spot signature in the time series of the pixel intensity from the natural pattern.

Since only a few authors proposed automated ways to detect defects and anomalies, there is also a lack of quantitative studies on actual detectability performances with different sensing methods and for different defect types and severities. Qualitative correlations (commonly based on visual analysis) between process signatures measured in situ and actual defects (e.g., pores and geometrical distortions) were presented and discussed by several authors, showing in some cases a good visual agreement with respect to ground truth data. Nevertheless, this is not sufficient to infer a probability-of-detection function, estimate false positive and false negative rates, or assess classification accuracies. Thus, further research in PBF-EB is needed to (1) combine proposed sensing methods with automated defect detection techniques, (2) characterize in situ monitoring performances in a quantitative way, and (3) investigate their suitability for actual in-line adoption with respect to computational efficiency, data storage needs, robustness in real production settings, etc.

Another aspect that deserves further attention and developments, as pointed out by various authors, regards in situ sensor calibration and data quality improvement. The specific nature of the PBF-EB imposes several challenges. Some sensing methods, like ELO imaging, are more robust than others to nuisance factors, but they allow capturing just a portion of the wide range of relevant information for process monitoring purposes. Optical imaging and NIR/IR video imaging open to complementary opportunities, but their implementation in PBF-EB suffers from many more limitations than in PBF-L. A variety of sensor installation setups have been proposed so far, but they can be further tuned and improved to achieve desired defect detection performances at different levels.

Various authors pointed out the potential of various in situ sensing and monitoring techniques not only for fast detection of defects, but also to support material development stages, reducing the experimental effort and costs. Indeed, in situ gathered data can be used as response variables to determine the printability window for a given material by screening out sets of process parameters that yield undesired patterns while samples are being produced, reducing the need for post-process inspections. However, no actual validation of in situ process optimization procedure has been presented so far. This is an additional and interesting application that deserves additional research and validation.

Eventually, an industrially relevant problem regards the capability of producing parts first-time-right and defect-free. Closed loop control has been investigated in PBF-L, where seminal and more recent studies showed the feasibility of preventing and/or mitigating unstable process states by adapting process parameters based on in-line measured quantities. Various methods reviewed in this study are potentially suitable to feed adaptive control loops in PBF-EB, but such potential has not been explored yet. Open architecture machines are needed to implement and validate this capability, and this still represents a limitation with respect to PBF-L. Indeed, several self-developed and open PBF-L prototype machines have spread in research laboratories, and they have been widely used as testbeds so far. Fully open PBF-EB systems, instead, are currently commercialized by only one company, and very few efforts have been made to develop open machines for research purposes.

In summary, despite various successful solutions that have been recently adopted by newcomer system developers, the literature devoted to in situ sensing and monitoring in PBF-EB is still less mature than the corresponding literature in PBF-L. Most promising sensing methods must still be combined with advanced data mining and machine learning solutions to make an impact on industrial production and qualification practices. In-line process optimization and closed-loop control represent two additional opportunities to leverage on in situ gathered data, either to aid material development or to achieve zero-defect capacities, but they represent fields where additional research and innovation efforts are required. The higher competitiveness expected in the PBF-EB market in the next years may give additional momentum to innovative solutions. Among them, in situ sensing, monitoring, and control may play a relevant role in fostering and consolidating the PBF-EB industrial adoption as well as to open and upscale new applications.

6 Conclusions

The layerwise production paradigm enables an unprecedented range of opportunities for in-line process monitoring, defect detection and control. Despite still far from the enormous number of studies devoted to the PBF-L process, the literature in PBF-EB is characterized by a variety of solutions characterized by different technology readiness levels. Some in situ sensing methods have reached a sufficient maturity to be installed by machine developers as embedded or optional equipment in their systems, while others still need additional development to enhance the quality of gathered

data and their suitability for industrial implementation. ELO imaging exhibits a high potential for the characterization of the surface pattern of solidified layers, which can be used to distinguish among different process conditions and detect deviations from a normal and stable process state. Good visual correlation between ELO maps and internal porosity structures have been presented too, which further highlight the potential of this technique for both process monitoring and in-line process optimization. NIR/IR video imaging has the complementary capability to capture spatial and temporal thermal gradients during the melting and cooling stages. This capability may allow one to predict the microstructural properties of the part, to detect anomalies in the heating and cooling profiles, to identify swelling phenomena and surface crack formations. Optical video imaging is also suitable to detect hot-spots, to analyse powder bed homogeneity, or to characterize the surface topography of the solidified layer when combined with a structured light source. The continuous growth of the literature on such in situ sensing methods still deserves additional research developments in the field of bid data analytics and machine learning for automated defect detection or process classification. Only few seminal works have been presented so far, and new developments are expected in the next years. In addition to in situ sensing and monitoring, adaptive and closed-loop control basically represents an unexplored field in PBF-EB, but the increased competitiveness in the sector together with new industrial adopters may pull novel solutions in this area too, aiming to meet rapidly changing market needs and to foster a new generation of smart PBF-EB systems.

Appendix

The procedure adopted in this study to collect the literature on in situ sensing and monitoring in PBF-EB was based on the following search methods:

- Search by keyword: Google Scholar and Scopus databases where searched using several different combinations of salient keywords including the following: “electron beam melting”, “electron beam”, “powder bed fusion”, “selective electron beam melting”, “additive manufacturing”, “monitoring”, “sensing”, “measurement”, “in situ”, “in-line”, “online”, “in-process”, “in-operando”, “defect detection”, “anomaly detection”, “error detection”, “process classification”, “machine learning”, “quality prediction”, “data analytics”, “statistical learning”, “statistical process monitoring”, “process control”.
- Search by author and research group: starting from (1) previously published reviews, (2) the results of our search by keywords, and (3) the authors’ knowledge of the research area, any additional or more recent papers from individual authors and the research groups they belong to were searched through direct links to research groups’ web-pages, Google Scholar personal pages, institutional websites.
- Search by references: for each found paper, a further search was performed by going through all cited papers therein and identifying the relevant ones.
- Search by citation: for each found paper, a further search was performed by going through all papers that cited it and identifying the relevant ones.
- Iteration of steps 1 to 4: once new papers and new authors were identified, the list of keywords was refined, more recent papers were searched, and all citations were explored to identify additionally relevant studies.
- Final screening phase: all papers selected through steps 1 to 5 were screened out based on their actual relevance to the topics included in this review.

Acknowledgements The research was supported by ACCORDO Quadro ASI-POLIMI “Attività di Ricerca e Innovazione” n. 2018-5-HH.0, collaboration agreement between the Italian Space Agency and Politecnico di Milano.

Funding Open access funding provided by Politecnico di Milano within the CRUI-CARE Agreement.

Declarations

Conflict of interest The authors certify that they have no affiliations with or involvement in any organization or entity with any financial interest, or non-financial interest in the subject matter or materials discussed in this manuscript.

References

1. Arnold C, Körner C (2021) Electron-optical in-situ metrology for electron beam powder bed fusion: calibration and validation. Meas Sci Technol 33(1):014001
2. Arnold C, Körner C (2021) In-situ electron optical measurement of thermal expansion in electron beam powder bed fusion. Addit Manuf 46:102213

3. Arnold C, Böhm J, Körner C (2020) In operando monitoring by analysis of backscattered electrons during electron beam melting. Adv Eng Mater 22(9):1901102
4. Arnold C, Breuning C, Körner C (2021) Electron-optical in situ imaging for the assessment of accuracy in electron beam powder bed fusion. Materials 14(23):7240
5. Arnold C, Pobel C, Osmanlic F, Körner C (2018) Layerwise monitoring of electron beam melting via backscatter electron detection. Rapid Prototyp J 24(8):1401–1406
6. Babu SS, Raghavan N, Raplee J, Foster SJ, Frederick C, Haines M, Dehoff RR (2018) Additive manufacturing of nickel superalloys: opportunities for innovation and challenges related to qualification. Metall Mater Trans A 49:3764–3780
7. Bäreis J, Semjatov N, Renner J, Ye J, Zongwen F, Körner C (2023) Electron-optical in-situ crack monitoring during electron beam powder bed fusion of the Ni-Base superalloy CMSX-4. Prog Addit Manuf 8(5):801–806
8. Boone N, Zhu C, Smith C, Todd I, Willmott JR (2018) Thermal near infrared monitoring system for electron beam melting with emissivity tracking. Addit Manuf 22:601–605
9. Breuning C, Arnold C, Markl M, Körner C (2021) A multivariate meltpool stability criterion for fabrication of complex geometries in electron beam powder bed fusion. Addit Manuf 45:102051
10. Chandrasekar S, Coble JB, Yoder S, Nandwana P, Dehoff RR, Paquit VC, Babu SS (2020) Investigating the effect of metal powder recycling in electron beam powder bed fusion using process log data. Addit Manuf 32:100994
11. Cordero PM, Mireles J, Ridwan S, Wicker RB (2017) Evaluation of monitoring methods for electron beam melting powder bed fusion additive manufacturing technology. Prog Addit Manuf 2:1–10
12. Croset G, Martin G, Josserond C, Lhuissier P, Blandin JJ, Dendievel R (2021) In-situ layerwise monitoring of electron beam powder bed fusion using near-infrared imaging. Addit Manuf 38:101767
13. Dehoff RR (2019) Electron beam melting technology improvements, CRADA final report, CRADA/NFE-12-04045
14. Dinwiddie RB, Dehoff RR, Lloyd PD, Lowe LE, Ulrich JB (2013) Thermographic in-situ process monitoring of the electron-beam melting technology used in additive manufacturing. In: Thermosense: thermal infrared applications XXXV, vol 8705. SPIE, pp 156–164
15. Escano LI, Clark SJ, Chuang AC, Yuan J, Guo Q, Qu M, Chen L (2022) An electron beam melting system for in-situ synchrotron X-ray monitoring. Addit Manuf Lett 3:100094
16. Eschey C, Lutzmann S, Zaeh M (2009) Examination of the powder spreading effect in electron beam melting (EBM). Solid freeform fabrication, TX, August, p 3–5
17. Fernandez A, Felice R, Terrazas-Nájera CA, Wicker R (2021) Implications for accurate surface temperature monitoring in powder bed fusion: using multi-wavelength pyrometry to characterize spectral emissivity during processing. Addit Manuf 46:102138
18. Fisher BA, Mireles J, Ridwan S, Wicker RB, Beuth J (2017) Consequences of part temperature variability in electron beam melting of Ti-6Al-4V. JOM 69:2745–2750
19. Fu Z, Körner C (2022) Actual state-of-the-art of electron beam powder bed fusion. Eur J Mater 2(1):54–116
20. Gong X, Cheng B, Price S, Chou K (2013) Powder-bed electron-beam-melting additive manufacturing: powder characterization, process simulation and metrology. In: Early career technical conference, Birmingham, AL, pp 55–66
21. Grasso M (2021) In situ monitoring of powder bed fusion homogeneity in electron beam melting. Materials 14(22):7015
22. Grasso M, Gallina F, Colosimo BM (2018) Data fusion methods for statistical process monitoring and quality characterization in metal additive manufacturing. Procedia Cirp 75:103–107
23. Grasso M, Remani A, Dickins A, Colosimo BM, Leach RK (2021) In-situ measurement and monitoring methods for metal powder bed fusion: an updated review. Meas Sci Technol 32(11):112001
24. Grasso M, Valsecchi G, Colosimo BM (2020) Powder bed irregularity and hot-spot detection in electron beam melting by means of in-situ video imaging. Manuf Lett 24:47–51
25. Ioannidou C, König HH, Semjatov N, Ackelid U, Staron P, Koerner C, Lindwall G (2022) In-situ synchrotron X-ray analysis of metal additive manufacturing: current state, opportunities and challenges. Mater Des 219:110790
26. Hankwitz JP, Ledford C, Rock C, O'Dell S, Horn TJ (2021) Electron beam melting of niobium alloys from blended powders. Materials 14(19):5536
27. Körner C (2016) Additive manufacturing of metallic components by selective electron beam melting—a review. Int Mater Rev 61(5):361–377
28. Le Roux L, Liu C, Ji Z, Kerfriden P, Gage D, Feyer F, Bigot S (2021) Automatised quality assessment in additive layer manufacturing using layer-by-layer surface measurements and deep learning. Procedia CIRP 99:342–347
29. Ledford C, Rock C, Tung M, Wang H, Schroth J, Horn T (2020) Evaluation of electron beam powder bed fusion additive manufacturing of high purity copper for overhang structures using in-situ real time backscatter electron monitoring. Procedia Manuf 48:828–838
30. Ledford C, Tung M, Rock C, Horn T (2020) Real time monitoring of electron emissions during electron beam powder bed fusion for arbitrary geometries and toolpaths. Addit Manuf 34:101365
31. Lee YS, Kirka MM, Dinwiddie RB, Raghavan N, Turner J, Dehoff RR, Babu SS (2018) Role of scan strategies on thermal gradient and solidification rate in electron beam powder bed fusion. Addit Manuf 22:516–527
32. Liu C, Le Roux L, Ji Z, Kerfriden P, Lacan F, Bigot S (2020) Machine Learning-enabled feedback loops for metal powder bed fusion additive manufacturing. Procedia Comput Sci 176:2586–2595
33. Liu Y, Blunt L, Zhang Z, Rahman HA, Gao F, Jiang X (2020) In-situ areal inspection of powder bed for electron beam fusion system based on fringe projection profilometry. Addit Manuf 31:100940
34. Liu Y, Zhang Z, Blunt L, Saunby G, Dawes J, Blackham B, Jiang X (2019) In-situ inspection system for additive manufacturing based on phase measurement profilometry. In: 19th international conference of the european society for precision engineering and nanotechnology, pp 324–327
35. McCann R, Obeidi MA, Hughes C, McCarthy É, Egan DS, Vijayaraghavan RK, Brabazon D (2021) In-situ sensing, process monitoring and machine control in laser powder bed fusion: a review. Addit Manuf 45:102058
36. Meng L, McWilliams B, Jarosinski W, Park HY, Jung YG, Lee J, Zhang J (2020) Machine learning in additive manufacturing: a review. Jom 72:2363–2377
37. Mireles J, Ridwan S, Morton PA, Hinojos A, Wicker RB (2015) Analysis and correction of defects within parts fabricated using powder bed fusion technology. Surf Topogr Metrol Prop 3(3):034002
38. Mireles J, Terrazas C, Gaytan SM, Roberson DA, Wicker RB (2015) Closed-loop automatic feedback control in electron beam melting. Int J Adv Manuf Technol 78:1193–1199
39. Mireles J, Terrazas C, Medina F, Wicker R (2013) Automatic feedback control in electron beam melting using infrared thermography. In: 2013 international solid freeform fabrication symposium. University of Texas at Austin

40. Nandwana P, Kirka MM, Paquit VC, Yoder S, Dehoff RR (2018) Correlations between powder feedstock quality, in situ porosity detection, and fatigue behavior of Ti-6Al-4V fabricated by powder bed electron beam melting: a step towards qualification. Jom 70(9):1686–1691
41. Oleff A, Küster B, Stonis M, Overmeyer L (2021) Process monitoring for material extrusion additive manufacturing: a state-of-the-art review. Prog Addit Manuf 6(4):705–730
42. Pagani L, Grasso M, Scott PJ, Colosimo BM (2020) Automated layerwise detection of geometrical distortions in laser powder bed fusion. Addit Manuf 36:101435
43. Pobel CR, Arnold C, Osmanlic F, Fu Z, Körner C (2019) Immediate development of processing windows for selective electron beam melting using layerwise monitoring via backscattered electron detection. Mater Lett 249:70–72
44. Price S, Cooper K, Chou K (2012) Evaluations of temperature measurements by near-infrared thermography in powder-based electron-beam additive manufacturing. In: 2012 international solid freeform fabrication symposium. University of Texas at Austin
45. Price S, Lydon J, Cooper K, Chou K (2014) Temperature measurements in powder-bed electron beam additive manufacturing. In: ASME international mechanical engineering congress and exposition, vol 46438. American Society of Mechanical Engineers, p V02AT02A002
46. Raplee J, Plotkowski A, Kirka MM, Dinwiddie R, Dehoff RR, Babu SS (2017a) Understanding the thermal sciences in the electron beam melting process through in-situ process monitoring. In: Nondestructive characterization and monitoring of advanced materials, aerospace, and civil infrastructure 2017, vol 10169. SPIE, pp 175–182
47. Raplee J, Plotkowski A, Kirka MM, Dinwiddie R, Okello A, Dehoff RR, Babu SS (2017) Thermographic microstructure monitoring in electron beam additive manufacturing. Sci Rep 7(1):1–16
48. Renner J, Breuning C, Markl M, Körner C (2022) Surface topographies from electron optical images in electron beam powder bed fusion for process monitoring and control. Addit Manuf 60:103172
49. Renner J, Grund J, Markl M, Körner C (2023) A ray tracing model for electron optical imaging in electron beam powder bed fusion. J Manuf Mater Process 7(3):87
50. Ridwan S, Mireles J, Gaytan SM, Espalin D, Wicker RB (2014) Automatic layerwise acquisition of thermal and geometric data of the electron beam melting process using infrared thermography. In: 2014 international solid freeform fabrication symposium. University of Texas at Austin
51. Rodriguez E, Medina F, Espalin D, Terrazas C, Muse D, Henry C, Wicker RB (2012) Integration of a thermal imaging feedback control system in electron beam melting. In: Proceedings of the solid freeform fabrication symposium, 2012
52. Rodriguez E, Mireles J, Terrazas CA, Espalin D, Perez MA, Wicker RB (2015) Approximation of absolute surface temperature measurements of powder bed fusion additive manufacturing technology using in situ infrared thermography. Addit Manuf 5:31–39
53. Scharowsky, T., Bauereiß, A., Singer, R., Körner, C. (2012). Observation and numerical simulation of melt pool dynamic and beam powder interaction during selective electron beam melting. In Proceedings of the solid freeform fabrication symposium. Springer, Switzerland
54. Scharowsky T, Osmanlic F, Singer R, Körner C (2014) Melt pool dynamics during selective electron beam melting. Appl Phys A 114(4):1303–1307
55. Schwerdtfeger J, Singer RF, Körner C (2012) In situ flaw detection by IR-imaging during electron beam melting. Rapid Prototyp J 18(4):259–263
56. Steed CA, Halsey W, Dehoff R, Yoder SL, Paquit V, Powers S (2017) Falcon: Visual analysis of large, irregularly sampled, and multivariate time series data in additive manufacturing. Comput Gr 63:50–64
57. Tang ZJ, Liu WW, Wang YW, Saleheen KM, Liu ZC, Peng ST, Zhang HC (2020) A review on in situ monitoring technology for directed energy deposition of metals. Int J Adv Manuf Technol 108:3437–3463
58. Terrazas-Nájera CA, Romero A, Felice R, Wicker R (2023) Multi-wavelength pyrometry as an in situ diagnostic tool in metal additive manufacturing: detecting sintering and liquid phase transitions in electron beam powder bed fusion. Addit Manuf 63:103404
59. Wang C, Tan XP, Tor SB, Lim CS (2020) Machine learning in additive manufacturing: state-of-the-art and perspectives. Addit Manuf 36:101538
60. Wang D, Zhao D, Liang X, Li X, Lin F (2023) Multiple stages of smoking phenomenon in electron beam powder bed fusion process. Addit Manuf 66:103434
61. Wong H (2020) Bitmap generation from computer-aided design for potential layer-quality evaluation in electron beam additive manufacturing. Rapid Prototyp J 26(5):941–950
62. Wong H (2020) Pilot investigation of surface-tilt and gas amplification induced contrast during electronic imaging for potential in-situ electron beam melting monitoring. Addit Manuf 35:101325
63. Wong H, Garrard R, Black K, Fox P, Sutcliffe C (2020) Material characterisation using electronic imaging for electron beam melting process monitoring. Manufact Lett 23:44–48
64. Wong H, Neary D, Jones E, Fox P, Sutcliffe C (2019) Benchmarking spatial resolution in electronic imaging for potential in-situ electron beam melting monitoring. Addit Manuf 29:100829
65. Wong H, Neary D, Jones E, Fox P, Sutcliffe C (2019) Pilot feedback electronic imaging at elevated temperatures and its potential for in-process electron beam melting monitoring. Addit Manuf 27:185–198
66. Wong H, Neary D, Jones E, Fox P, Sutcliffe C (2019) Pilot capability evaluation of a feedback electronic imaging system prototype for in-process monitoring in electron beam additive manufacturing. Int J Adv Manuf Technol 100:707–720
67. Wong H, Neary D, Shahzad S, Jones E, Fox P, Sutcliffe C (2019) Pilot investigation of feedback electronic image generation in electron beam melting and its potential for in-process monitoring. J Mater Process Technol 266:502–517
68. Ye J, Renner J, Körner C, Fu Z (2023) Electron-optical observation of smoke evolution during electron beam powder bed fusion. Addit Manuf 70:103578
69. Yoder S, Morgan S, Kinzy C, Barnes E, Kirka M, Paquit V, Babu SS (2018) Characterization of topology optimized Ti-6Al-4V components using electron beam powder bed fusion. Addit Manuf 19:184–196
70. Yoder S, Nandwana P, Paquit V, Kirka M, Scopel A, Dehoff RR, Babu SS (2019) Approach to qualification using E-PBF in-situ process monitoring in Ti-6Al-4V. Addit Manuf 28:98–106
71. Zhao DC, Lin F (2021) Dual-detector electronic monitoring of electron beam selective melting. J Mater Process Technol 289:116935